Applied Catalysis A: General 469 (2014) 357–366

Contents lists available at ScienceDirect

Applied Catalysis A: General

journal homepage: www.elsevier.com/locate/apcata

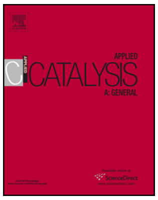

Experimental investigation of ethylene hydroformylation to propanal on Rh and Co based catalysts

N. Navidi, J.W. Thybaut*, G.B. Marin

Laboratory for Chemical Technology, Chemical Engineering Department, Ghent University, Technologiepark 914, Ghent 9052, Belgium

ARTICLE INFO

Article history:
Received 25 June 2013
Received in revised form 9 September 2013
Accepted 8 October 2013
Available online 18 October 2013

Keywords:
Heterogeneous catalysis
Ethylene
Hydroformylation
Hydrogenation
Rhodium
Cobalt

ABSTRACT

Intrinsic hydroformylation kinetics have been measured in a high-throughput kinetic test setup at temperatures varying from 448 to 498 K, with the total pressure ranging from 1 to 3 MPa. A gaseous feed containing CO, C_2H_4 and H_2 was used with space times varying from 2.7 kg_{cat} s/$mol_{C_2H_4,in}$ to 149 kg_{cat} s/$mol_{C_2H_4,in}$. Three catalysts have been investigated, i.e., 5%Rh on Al_2O_3, 1%Co on Al_2O_3 and 0.5%Co–0.5%Rh on Al_2O_3. The main products observed were ethane, propanal and propanol. The Rh catalyst showed the highest hydroformylation and hydrogenation site time conversions in the investigated range of operating conditions. Moreover it was found on all investigated catalysts that the hydrogenation activation energy was about 15–20 kJ mol^{-1} higher than that for hydroformylation. On the Rh catalyst, higher ethylene feed concentrations have a more pronounced effect on CO conversion and production of propanal and propanol compared with an increase in the inlet concentration of the other reactants.

1. Introduction

The ever increasing crude oil price has led to the exploration of alternative feeds such as natural gas and, correspondingly, new processes for the production of hydrocarbon chemicals. Hydroformylation, or oxo synthesis, that was discovered by the German scientist Otto Roelen in 1938, is an important process for production of aldehydes. The latter may play a key role in the upgrading and/or separation of alkenes produced via alternative routes such as oxidative coupling of methane or methanol to olefins. Hydroformylation catalysts generally also exhibit double bound hydrogenation which results in reactant alkene conversion into the corresponding alkane as well as product aldehyde conversion into alcohols [1]. Typical hydroformylation products are in the carbon number range from 3 to 19, the reactant alkene being selected based on the desired product aldehyde.

Aldehydes are useful intermediates in the production of valuable products such as alcohols, carboxylic acids, amines, and diols. More recently, hydroformylation is also widely applied in the fine chemicals and pharmaceutical industry for the production of drugs, vitamins, herbicides and perfumes [2,3].

At 373 K, ethylene hydroformylation is a spontaneous, exothermic reaction with $\Delta H^\circ = -129.0$ kJ mol^{-1} and $\Delta G^\circ = -56.9$ kJ mol^{-1}. Due to the high activation energies involved, the reaction rate remains rather low, however [4].

In principle, all the transition metals capable of forming carbonyls, such as Rh, Co, Ir, Ru,. are potential hydroformylation catalysts. The order of activity from the most to the least active metal, is as follows: Rh > Co > Ir, Ru > Os > Pt > Pd > Fe > Ni [5]. Cobalt complexes had been the main industrial hydroformylation catalysts until the early 1970s, i.e., prior to the commercialization of rhodium based catalysts. Since then, cobalt catalysts for hydroformylation have been replaced in almost all major plants by the more advantageous rhodium catalysts despite the higher price of the noble metal. This substitution became feasible because the high price of rhodium was offset by cheaper equipment, increased catalyst activity, and a generally higher selectivity and efficiency.

Commercially, homogeneous Co or Rh complexes are typically applied at temperatures ranging from as low as 360 K up to 573 K [6,7]. The homogeneous character of industrial process configurations leads to inherent operational problems such as difficulties in catalyst separation from products, expensive metal losses and corrosivity of catalytic solutions. The successful implementation of an active and stable heterogeneous hydroformylation catalyst would allow avoiding these drawbacks. Although the research into heterogeneously catalysed hydroformylation is in an early stage, a wide range of research activities has been performed on experimental heterogeneous hydroformylation with various reactants, catalysts and operation conditions [8–17].

Reaction mechanism elucidation is an important subject in the reported heterogeneous hydroformylation studies. The most

---

* Corresponding author. Tel.: +32 9 331 17 52.
E-mail address: Joris.Thybaut@UGent.be (J.W. Thybaut).

0926-860X/$ – see front matter © 2013 Elsevier B.V. All rights reserved.
http://dx.doi.org/10.1016/j.apcata.2013.10.019

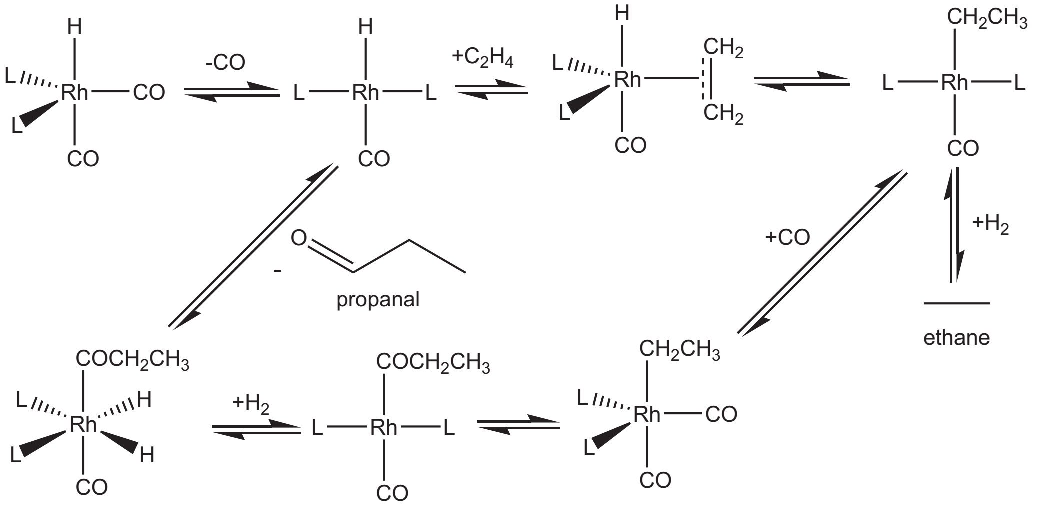

Fig. 1. Wilkinson mechanism for heterogeneous hydroformylation [18].

referenced hydroformylation reaction mechanism was that proposed by Wilkinson and his co-authors [18]. In essence, this mechanism comprises 8 elementary steps, see Fig. 1, i.e., 1: carbon monoxide desorption, 2: alkene chemisorption, 3: hydride addition (towards a metal alkyl), 4: hydrogenation to ethane (side reaction), 5: carbon monoxide molecular chemisorption, 6: carbon monoxide insertion into the metal alkyl bond, 7: hydrogen chemisorption and 8: aldehyde elimination.

The present work concentrates on heterogeneous ethylene hydroformylation on a series of Rh and Co based catalysts. Gas phase experimentation was performed in a high-throughput kinetics setup to compare the Rh and Co catalysts and to investigate the effect of the operation conditions on the main and by product formation rates on these catalysts. We aim at a fundamental analysis both in terms of operating conditions as well as in terms of catalyst properties and how they could be potentially enhanced. Even if the catalysts investigated give only moderate oxygenate yields, the mechanistic investigation provides key insight into the corresponding reaction mechanism that may be exploited in further catalyst design.

2. Experimental

2.1. Catalysts preparation

In order to provide a good comparison of the Co and Rh catalysts which are used most frequently in industrial homogeneous hydroformylation, 5%Rh deposited on Al_2O_3, 1%Co deposited on Al_2O_3 and 0.5%Rh–0.5%Co deposited on Al_2O_3 catalysts, provided by Johnson Matthey, have been investigated in this work. They were received as powders, pressed into flakes and subsequently crushed and sieved to retain a fraction with a diameter between 0.3 and 0.5 mm. The catalysts were reduced in situ at 673 K in order to convert them into their active form.

2.2. Catalyst characterisation

The total surface area (BET) of each catalyst was measured using a Micromeritics Gemini equipment. The crystallinity of the samples was investigated via X-ray diffraction (XRD) measurements with a Siemens Diffractometer Kristalloflex D5000, Cu Kα radiation, in the 2θ range 4–90° step.

The metal loading and corresponding particle size were too low for retrieving useful information from temperature programme reduction (TPR), temperature programmed desorption (TPD) nor from X-ray diffraction (XRD) measurements. As a result, transmission electron microscopy (TEM) was performed to determine metal particle sizes and achieve information about the distribution and configuration of these metal particles on the surface of the three investigated catalysts. TEM samples were prepared by applying simple immersion of a carbon-support film on a nickel grid into the catalyst powder. The excess powder was shaken off carefully afterwards. Catalyst particles that had adhered to the carbon film were investigated by different TEM modes: conventional and high resolution (HR) TEM, electron diffraction, STEM, EDX and electron energy loss spectroscopy (EELS). A JEOL, JEM2200FS-Cs-corrected microscope was used. This microscope was operated at 200 kV and equipped with Schottky-type FEG, EDX JEOL JED-2300D and JEOL in-column omega filter. Secondary X-ray fluorescence from the analytical sample holder was eliminated by means of a beryllium retainer. However, Ni-peaks were detected in the EDX spectra due to secondary fluorescence from the Ni support grid. EEL spectra were obtained in STEM spot mode using an electron probe of 1.0 nm and objective aperture angular size of 6 mrad.

2.3. Intrinsic kinetics measurements

Gas phase hydroformylation measurements have been performed in a high-throughput kinetics test setup, see Fig. 2. This setup, which was constructed by Zeton B.V., consists essentially of three separate sections: a feed section, a reactor section and an analysis section. The setup consists of eight parallel reactors that are positioned per pair in a split type bronze furnace, i.e., reactor temperature and pressure are controlled per reactor pair. Each reactor has three gas feed lines and one liquid feed line. Each of these lines has an individual mass flow controller. The reactor tubes are made of AISI 316 cold worked steel with 890 mm height and 11 mm internal diameter and are capable of operating up to 600 °C and 15 MPa, i.e., far beyond the operating range as required for hydroformylation. A three-zone reactor temperature control is established by electrical heating within the bronze furnace, the catalyst being situated at the bottom of the second zone and the top of third zone. The reactants were mixed before entering the reactor from the top in the central axis. The pressure in the reactor was generated by means of back pressure. The operation of the setup was controlled by means of Labview software.

Between 1 and 10 g of pelletised catalyst was diluted with an identical mass of inert material prior to loading into the reactor

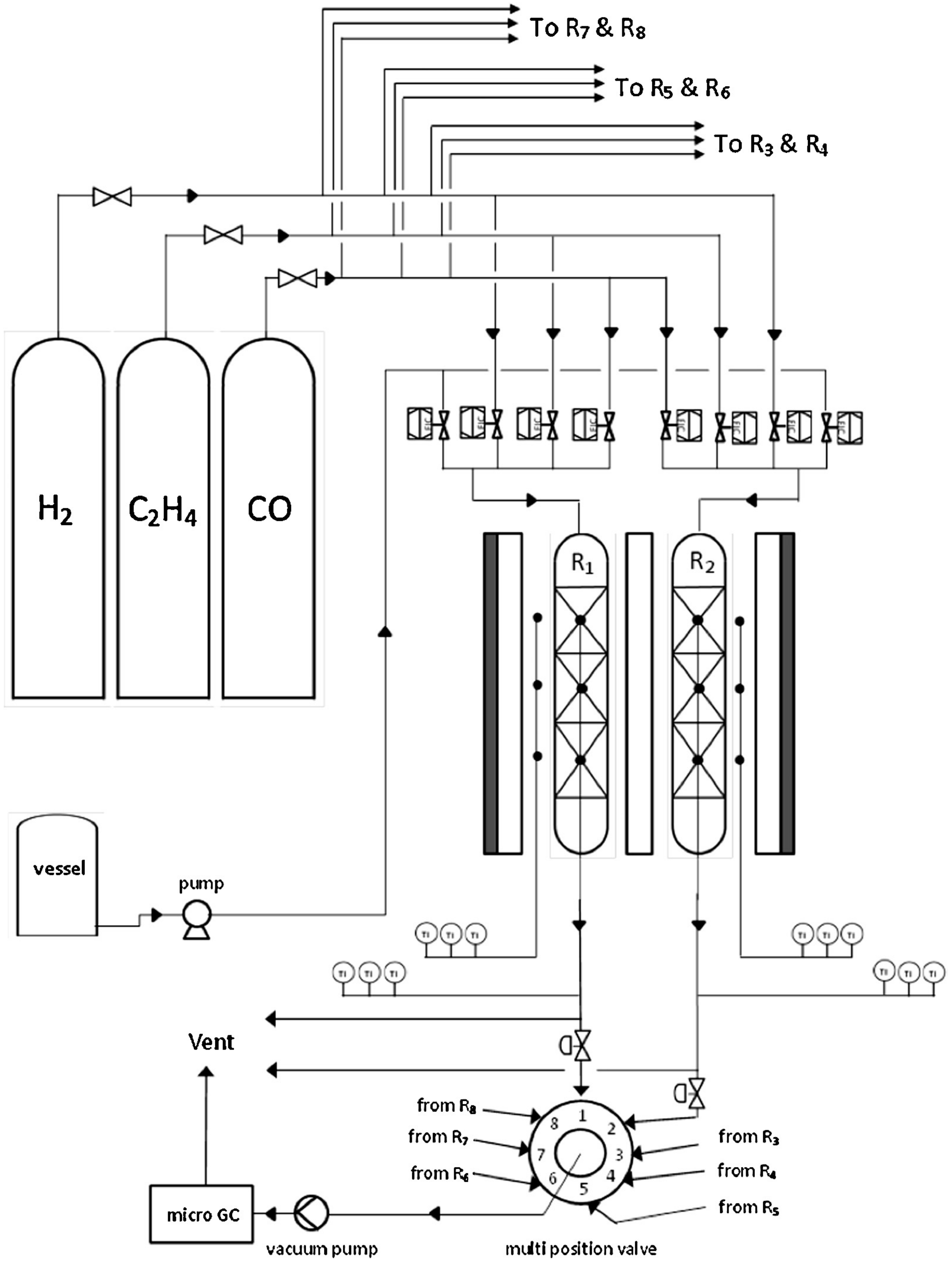

Fig. 2. Schematic overview of the high-throughput kinetics test setup.

Table 1
Operating conditions and catalysts used in the experimental investigation of the ethylene hydroformylation kinetics.

Catalyst	Temperature (K)	Pressure (MPa)	Space time range ($kg_{cat}\ s/mol_{C_2H_4,in}$)	$CO/C_2H_4/H_2$
Catalyst performance				
$5\%Rh/Al_2O_3$ $1\%Co/Al_2O_3$ $0.5\%Rh/0.5\%Co/Al_2O_3$	473	2	5.4–149	1/1/1
Temperature and pressure effect				
$5\%Rh/Al_2O_3$ $1\%Co/Al_2O_3$	448–498	1–3	2.7–149	1/1/1
Inlet composition effect				
$5\%Rh/Al_2O_3$	473	2	2.7–80	1/1/1; 2/1/1 1/2/1; 1/1/2

tubes of the high-throughput setup. Table 1 presents the operating conditions applied during the corresponding experiments, aiming to compare the performance of the mentioned catalysts and to investigate temperature, pressure and inlet composition effects on the hydroformylation reaction behaviour.

Online effluent analysis was performed with a four channel Agilent 3000 micro gas chromatograph equipped with thermal conductivity detectors (TCDs). Hydrogen, and carbon monoxide were analysed on a molar sieve 5A PLOT column of 10 m length and 0.32 inner diameter with a film thickness of 12 μm, while ethylene and ethane are detected on a PLOT U column of 8 m length and 0.32 inner diameter with a film thickness of 30 μm. Heavy hydrocarbons can be detected in an Alumina PLOT column of 10 m length and 0.32 mm inner diameter with a film thickness of 8 μm. Propanal, propanol and other oxygenates are only detected on the OV-1 column of 10 m length and 0.15 mm inner diameter with a film thickness of 2 μm. Argon was added as an internal standard for the purpose of mass balance verification. The maximum error of mass balance was less than 10% while most of the error values were below 5%. The elemental balances were also verified and the deviations were in line with those on the total mass balance. The conversions and product molar flow rates were calculated using calibration factors as reported by Dietz [19].

Long-term catalyst stability was assessed by repeating a reference experiment at regular time intervals, i.e., one every few days. Typically the catalyst activity could be maintained for 3–4 weeks, after which the catalyst was replaced by a fresh sample. The selectivity towards a product P, S_p, was defined as the number of moles transformed into that product, F_p, compared to the total number of ethylene moles converted:

$$S_p = \frac{F_p}{F_{C_2H_4,0} - F_{C_2H_4}} \tag{1}$$

In order to compare the performance of the mentioned catalysts under identical experimental conditions the conversions were reported versus the so-called site time, which is obtained from the space time by accounting for the metal loading and the fraction of exposed metal atoms, as well as for atomic mass.

$$\text{site time} = \frac{\text{space time} \times \text{metal loading}}{M_M} \times \text{FE} \tag{2}$$

The fraction exposed was obtained from the relation between the particle size and dispersion as shown in Eqs. (3) and (4) [20].

$$d_{rel(VS)} = \frac{d_{VS}}{d_{at}} = \frac{5.01}{\text{FE}} \quad \text{for FE} < 0.2 \tag{3}$$

$$d_{rel(VS)} = \frac{d_{VS}}{d_{at}} = \frac{3.32}{\text{FE}^{1.23}} \quad \text{for } 0.2 \leq \text{FE} \leq 0.92 \tag{4}$$

It was verified by using the proper correlations, that at the selected operating conditions so-called intrinsic kinetics are measured, i.e., the observations are not affected by mass or heat transfer limitations [21]. Of course, upon extrapolation towards the industrial scale, potential mass and heat transport effects must be accounted for.

3. Heterogeneous ethylene hydroformylation reaction network

The most generally reported products for ethylene hydroformylation, in descending order of importance, are ethane, propanal, propanol and small amount of C_{3+} hydrocarbon products [7,10,12,13,16,22]. According to Henrici-Olivé and Olivé [23] the key difference between the homogeneous and the heterogeneous reactions is the presence of a free, mobile and very reactive hydrido-metal species in solution. They reported that the transformation of the acyl-metal species to the aldehyde, see steps 6 and 7 in Fig. 1, proceeds through reaction with a second catalyst species in homogeneous media while in heterogeneous media the oxidative addition of molecular hydrogen to an acyl-metal species is the only way for aldehyde formation [7,23].

It is accepted today that Wilkinson's mechanism is the most likely one in hydroformylation [3,22,24]. In this mechanism, it is assumed that carbon monoxide does not dissociate on the catalyst surface. The absence of a CO dissociation step in ethylene hydroformylation on silica supported rhodium catalysts is also reported by Hanaoka et al. [14]. These authors observed that the CO insertion to an alkyl species to form an acyl species is the key step for hydroformylation that controls the selectivity towards oxygenated products.

Considering the above discussion, a reaction mechanism for ethylene heterogeneous hydroformylation is proposed in what follows, see Fig. 3. It includes two parallel reaction pathways, starting from a metal bound alkyl that is obtained after ethylene chemisorption on the metal surface. The first, and in hydroformylation desired pathway, involves CO insertion and leads to aldehyde or alcohol formation. The second of the parallel pathways is ethylene hydrogenation into ethane. In this mechanism, the same hydrogen and ethylene surface species are involved in the formation of both ethane and propanal.

The potential presence of propene and higher carbon number alkenes, alkanes, aldehydes and alcohols can be explained by CO bond dissociation in the produced aldehydes or by CO bond dissociation and subsequent C hydrogenation to methylene prior to insertion in a metal alkyl species, as it may occur in Fischer–Tropsch synthesis [25–27]. Not only historically, but also mechanistically, heterogeneously catalysed hydroformylation is very closely related to Fischer–Tropsch synthesis. In fact, the reaction of ethylene with syngas has already been used as a probe reaction to study the activity and selectivity in the Fischer–Tropsch process on supported transition metals [9].

Because this comprehensive mechanism allows describing the formation of all hydroformylation products observed in this work, i.e., aldehydes and alcohols, as well as ethane, it is further used in the assessment of the kinetic data.

4. Results and discussion

4.1. *Catalyst characterisation*

4.1.1. *BET Surface area*

The BET surface areas for the investigated catalysts are reported in Table 2. Only minor differences are observed between the catalysts considered, indicating that the Al_2O_3 support is governing the observed surface areas. Nevertheless, as may have been expected, the catalyst with highest metal loading exhibits the lowest surface area.

4.1.2. *TEM analysis*

The presence of Rh and Co on the investigated catalyst samples was confirmed first by scanning transmission electron microscopy (STEM) coupled with energy dispersive X-ray (EDX). The corresponding pictures are given in Fig. 4a for 5%Rh on Al_2O_3, Fig. 4 for

Table 2
BET surface area for the Rh and Co based catalysts used in this work.

Catalyst	BET surface area (m^2/g)
5%Rh/Al_2O_3	120
0.5%Rh–0.5%Co/Al_2O_3	147
1%Co/Al_2O_3	143

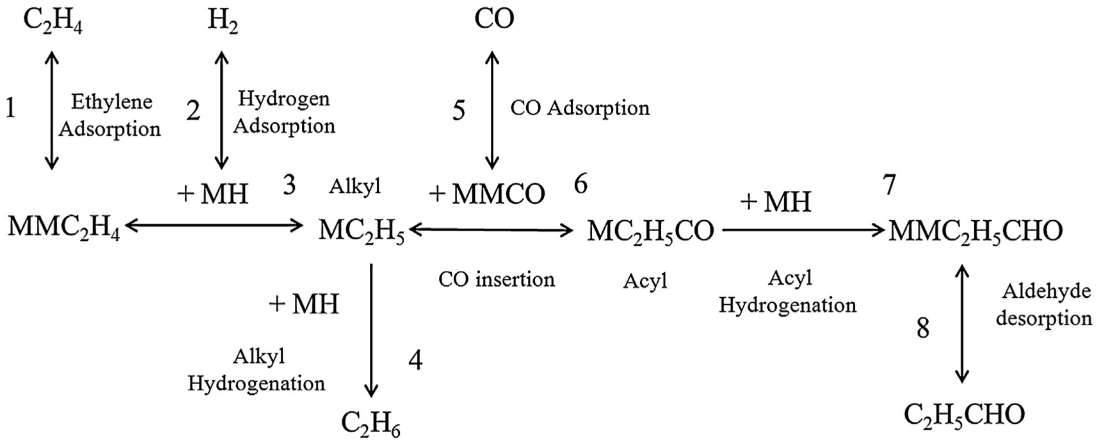

Fig. 3. Proposed reaction mechanism for ethylene hydroformylation to propanol [22].

1%Co on Al_2O_3 and in Fig. 4 for 0.5%Rh/0.5%Co on Al_2O_3. 5%Rh on Al_2O_3, see Fig. 4a, has well dispersed particles with a small size, i.e., 2 nm, resulting in a high fraction of exposed Rh.

The images show a, still small yet significantly larger particle size, i.e., 11 nm, for the 1%Co catalyst while the 0.5%Rh/0.5%Co contained large Rh clusters, i.e., 20–50 nm, but small Co particles, i.e., 4.3 nm. In other words, while Rh was finely dispersed on the 5%Rh catalyst and Co was somewhat more poorly dispersed on the 1%Co catalyst, the Rh dispersion on the 0.5%Rh/0.5%Co catalyst was extremely poor, while the Co dispersion was again better on this latter catalyst. The measured particle sizes and corresponding fractions exposed are reported in Table 3.

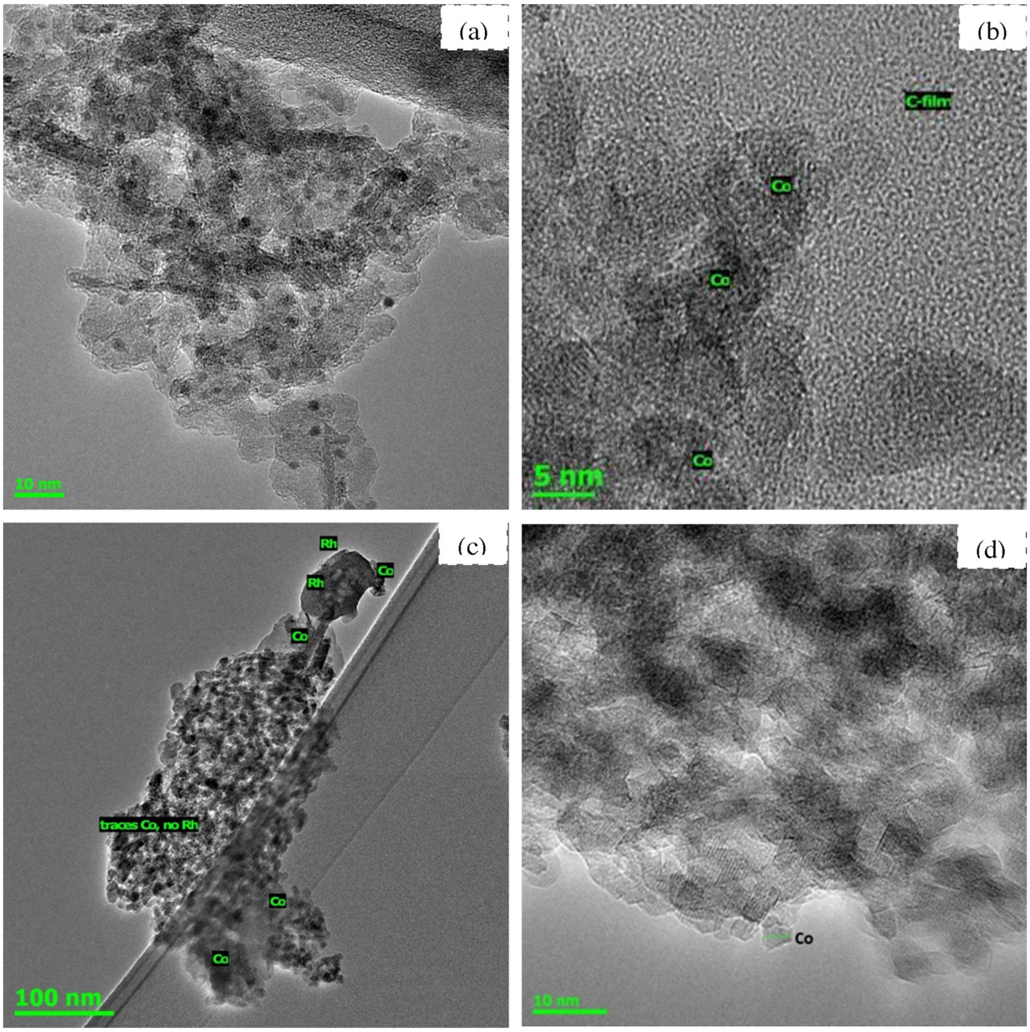

Fig. 4. TEM images for: (a) 5%Rh on Al_2O_3 catalyst, (b) 1%Co on Al_2O_3 catalyst, (c and d) 0.5%Rh/0.5%Co on Al_2O_3 catalyst.

Table 3
Particle size, fraction of exposed metal and accessible metal atoms for the Rh and Co based catalysts used in this work.

Catalyst	Particle size (nm) TEM	Fraction of exposed metal (%)	Accessible metal atoms (mol/$g_{cat.}$)
$5\%Rh/Al_2O_3$	2	51.1	2.4757×10^{-4}
$1\%Co/Al_2O_3$	11	12.4	0.2098×10^{-4}
$0.5\%Rh–0.5\%Co/Al_2O_3$	4.3 for Co 35 for Rh	28.1 for Co 3.8 for Rh	0.2575×10^{-4}

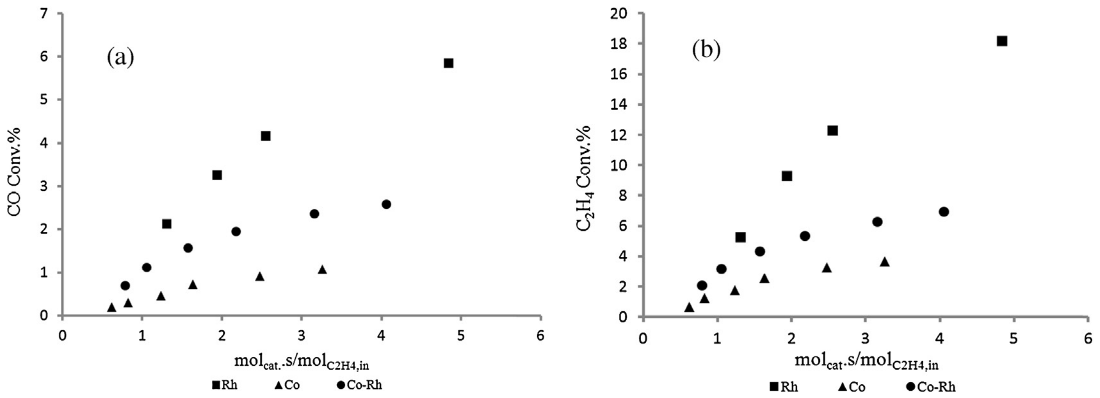

Fig. 5. (a) CO conversion versus molar site time and (b) C_2H_4 conversion versus molar site time. Reaction conditions: temperature 473 K; pressure, 2.0 MPa; gas inlet composition, C_2H_4:CO:H_2:Ar = 30:30:30:10), 2 MPa.

4.2. Catalytic performance

Fig. 5 shows the observed CO and C_2H_4 conversion as a function of the site time at 473 K and 2 MPa. The CO and C_2H_4 site time conversions that were calculated based on the results presented in these figures are reported in Table 4.

5%Rh on Al_2O_3 exhibited the highest site time conversions in the entire range of operating conditions, while the lowest site time conversions were obtained on 1%Co on Al_2O_3.

Based on the site time conversions obtained with the monometallic catalysts and the knowledge of the fractions exposed on the bimetallic catalyst, see Table 3, an expected site time conversion on this bimetallic catalyst amounting to 0.00429 $mol_{CO,\ converted}/mol_{cat.\ atoms}/s$ was calculated, which is lower than the experimentally observed site time conversion. Giving the large Rh particle size on the 0.5%Rh/0.5%Co on Al_2O_3 catalyst, the higher than expected site time conversions observed on the latter catalyst are attributed to the finely dispersed Co. Indeed, particle size effects, also denoted as structure sensitivity, have already been reported in hydroformylation [8,14] as well as in Fischer–Tropsch synthesis [28].

The product distribution on these catalysts are reported in Table 5. The 5%Rh on Al_2O_3 catalyst exhibited the highest selectivity for oxygenates among these catalysts. The 0.5%Rh/0.5%Co on Al_2O_3 catalyst also exhibits a higher selectivity for oxygenated compounds compared to the Co catalyst, which can, again, be related to the differences in Co particle size on the catalyst surface. The previously reported particle size effects [8,14] particularly concern the CO insertion activity rather than the hydrogenation activity and, hence, result in an increase of the oxo-selectivity.

A minor presence of methane in the product stream can be the result of CO chemisorption, dissociation and hydrogenation to methane. The selectivity of methane never exceeded 2% in this work. Upon insertion of an intermediate methylene species into a metal alkyl species, the latter will grow, as it occurs in the Fischer–Tropsch synthesis reaction mechanism. Of course, CO bond dissociation after a prior insertion in a metal alkyl species may also explain the formation of heavier hydrocarbons [29]. The amount of methane and C_{3+} hydrocarbon products on the tested catalysts barely exceeded 5%, which is sufficiently low to assume that practically all of the converted CO ended up in hydroformylation products, i.e., propanal or propanol. Hence, the selected

Table 4
Site time conversions obtained on the Rh and Co based catalysts used in the present work at 473 K, 2.0 MPa and equimolar $C_2H_4/CO/H_2$ gas inlet composition.

Catalyst	CO site time conversion ($mol_{CO,\ converted}/mol_{cat.\ atoms}/s$)	C_2H_4 site time conversion ($mol_{C_2H_4,converted}/mol_{cat.\ atoms}/s$)
$5\%Rh/Al_2O_3$	0.01356	0.04071
$1\%Co/Al_2O_3$	0.00359	0.01486
$0.5\%Rh–0.5\%Co/Al_2O_3$	0.00746	0.02626

Table 5
Product distribution obtained on the Rh and Co based catalysts used in the present work at 478 K, 2.0 MPa and equimolar $C_2H_4/CO/H_2$ gas inlet composition.

Catalyst	Product selectivities (%)					
	CH_4	C_2H_6	C_3H_6	$C_4H_8 + C_4H_{10}$	C_3H_5OH	C_3H_7OH
$5\%Rh/Al_2O_3$	0.4	62.4	0.6	1.6	28	7
$1\%Co/Al_2O_3$	1.1	71.7	1.3	1.9	18	6
$0.5\%Rh–0.5\%Co/Al_2O_3$	0.7	66.8	1	2.2	19.6	9.7

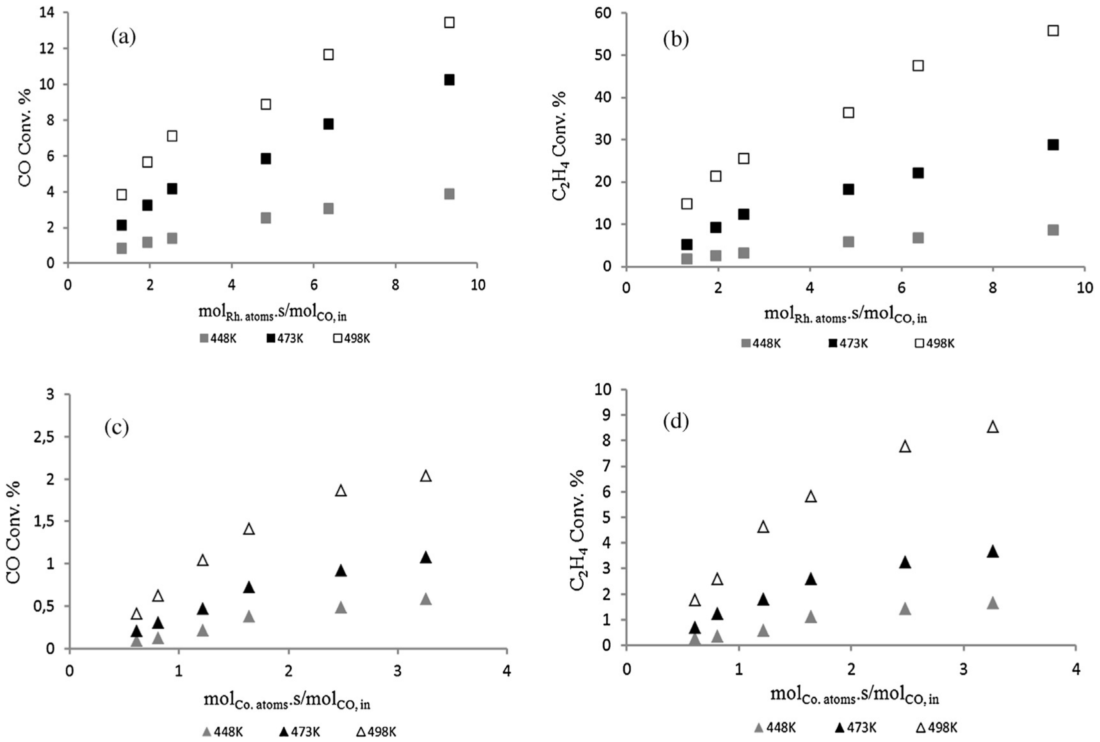

Fig. 6. (a) CO conversion versus site time on 5%Rh on Al_2O_3, (b) C_2H_4 conversion versus site time on 5%Rh on Al_2O_3, (c) CO conversion versus site time on 1%Co on Al_2O_3, and (d) C_2H_4 conversion versus site time on 1%Co on Al_2O_3. Reaction conditions: temperature, 448, 473 and 498 K; pressure, 2.0 MPa, gas inlet composition, C_2H_4:CO:H_2:Ar = 30:30:30:10.

mechanism for ethylene hydroformylation, see Fig. 3, can appropriately describe the reaction.

4.2.1. Temperature effect

The temperature and pressure effect on the hydroformylation rate were investigated on the 5%Rh on Al_2O_3 and 1%Co on Al_2O_3 catalysts. The temperature effect on CO and C_2H_4 conversion and, hence, the ethylene hydroformylation and hydrogenation rates on the Rh and Co catalyst at a fixed pressure of 2 MPa is presented in Fig. 6.

The correspondingly calculated site time conversions are represented in Fig. 7 as a function of the inverse of the temperature. A temperature increase leads to a more pronounced increase of the C_2H_4 site time conversion than of the CO site time conversion on both tested catalysts. Correspondingly, the apparent activation energy for ethane formation as determined from the Arrhenius diagram presented in Fig. 7 exceeds that for propanal formation on both tested catalysts by 15–20 kJ mol^{-1}. Hence, as it can be seen in Fig. 8, a temperature increase has a negative effect on the selectivity towards oxygenated compounds on both catalysts. For example by increasing the temperature from 448 K to 498 K on 5%Rh on Al_2O_3 at 2 MPa, the oxygenates selectivity decreased from 0.45 to 0.26. Similar observations are encountered in the literature [9,12], where increased ethane selectivities with the temperature were reported. It was observed by Balakos and Chuang [9], that in heterogeneous ethylene hydroformylation on 4%Rh/SiO_2 with increasing the temperature from 483 K to 573 K the hydroformylation selectivity, defined as $TOF_{propanal}/TOF_{C_2H_6}$, decreased from 0.136 to 0.039. Hence, a good hydroformylation catalyst should exhibit a high activity at lower operating temperatures to avoid a too significant loss in product selectivity.

The more pronounced temperature effect on hydrogenation than on hydroformylation can be assessed using the previously discussed heterogeneous ethylene hydroformylation mechanism, see Fig. 3: with increasing temperature, adsorbed C_2H_4 molecules apparently exhibit a higher affinity towards reductive elimination into ethane, step 4, than reacting with adsorbed CO molecule, step 6, on the catalyst surface. This can be related to the expected evolution in the hydrogen and CO surface concentrations. Because the chemisorption heat of CO is typically about the double of that of hydrogen [30], the CO concentration will decrease much faster with increasing temperature than the hydrogen concentration. As a

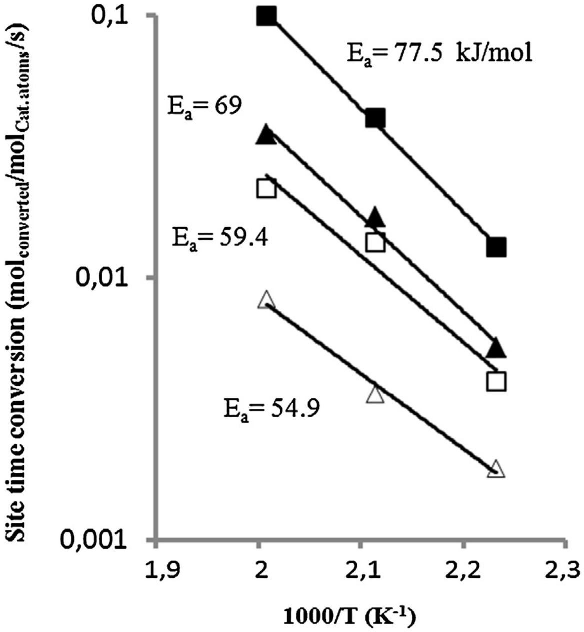

Fig. 7. Relation between space-time yield and temperature for hydrogenation rate on Rh (■) and Co (▲) and hydroformylation rate on Rh (□) and Co (△).

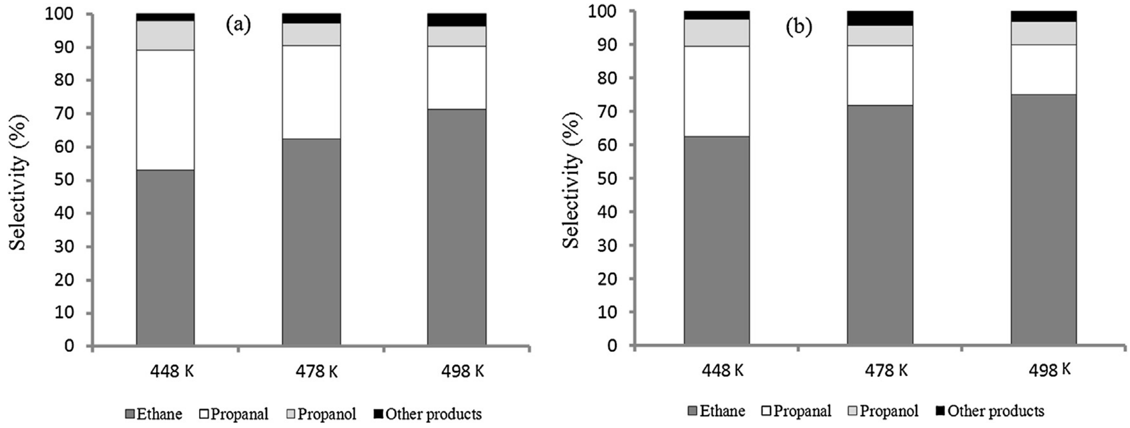

Fig. 8. Product selectivities at 2.0 MPa and equimolar C_2H_4/CO/H_2 gas inlet composition (a) on the 5%Rh/Al_2O_3 catalyst and (b) the 1%Co/Al_2O_3 catalyst.

result, the relative importance of hydrogenation in the overall ethylene conversion will increase at the expense of hydroformylation.

4.2.2. Pressure effect

The pressure effect on the CO and ethylene conversion as a function of the site time at 473 on the Rh and Co catalyst is shown in Fig. 9. All conversions and consequently hydroformylation and hydrogenation rates increase with the total pressure to a similar extent. A slightly more pronounced enhancement of the hydroformylation rate compared to the hydrogenation rate may be discerned, in agreement with the literature [13]. At a higher total pressure also the surface concentrations on the metal particles are correspondingly higher. The slightly increased oxygenates selectivity indicates that in particular the CO surface concentration has increased.

4.2.3. Inlet composition effect

The effect of variations in C_2H_4, CO and H_2 inlet composition on the CO and C_2H_4 conversion, was investigated on 5%Rh on Al_2O_3 and is reported in Fig. 10. As it can be observed from Fig. 10a, the CO conversion and, hence, the hydroformylation rate, increases with the ethylene inlet concentration. Also the C_2H_4 conversion by hydrogenation is enhanced by increasing its inlet concentration, see Fig. 10b. This can be understood when C_2H_4 concentrations on the catalyst surface are rather low and, hence, when an increasing C_2H_4 surface concentration has a negligible impact on the other surface concentrations. Increasing the inlet H_2 concentration leads

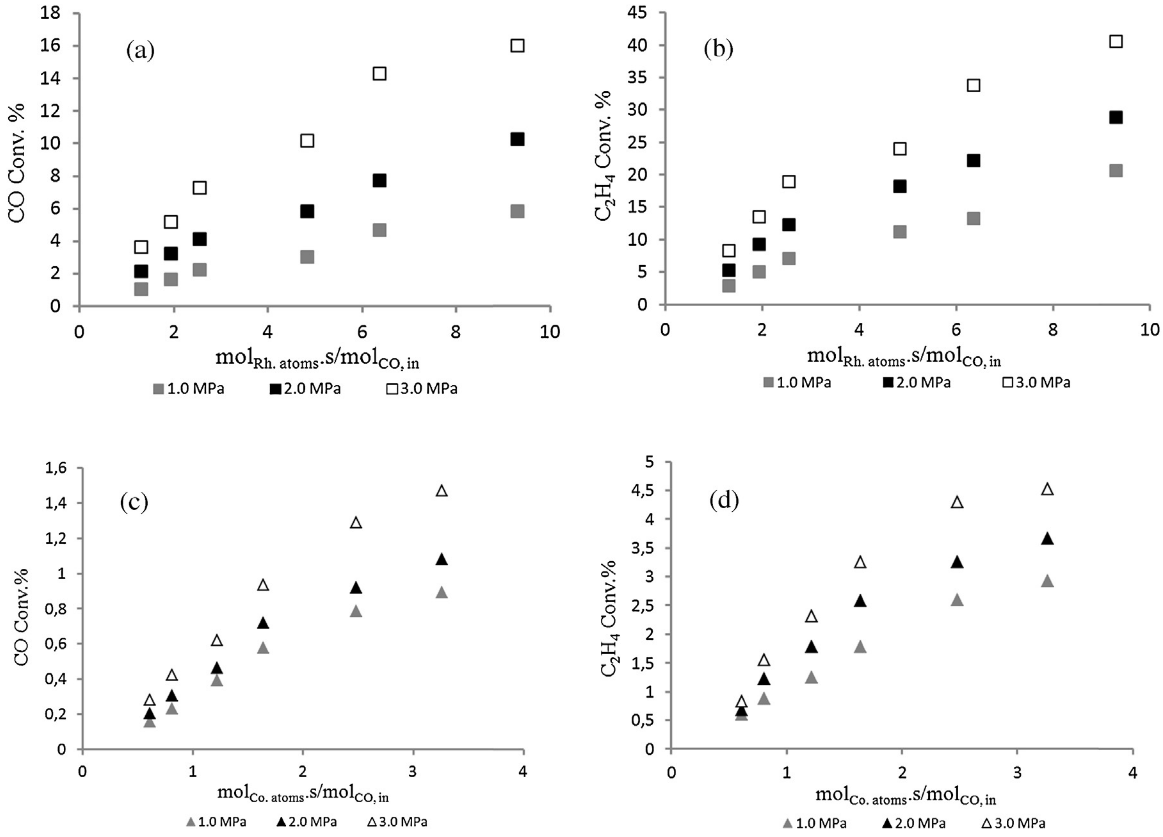

Fig. 9. (a) CO conversion versus site time on 5%Rh on Al_2O_3, (b) C_2H_4 conversion versus site time on 5%Rh on Al_2O_3, (c) CO conversion versus site time on 1%Co on Al_2O_3 and (d) C_2H_4 conversion versus site time on 1%Co on Al_2O_3 at different total pressures. Reaction conditions: temperature, 473 K; gas inlet composition, C_2H_4:CO:H_2:Ar = 30:30:30:10.

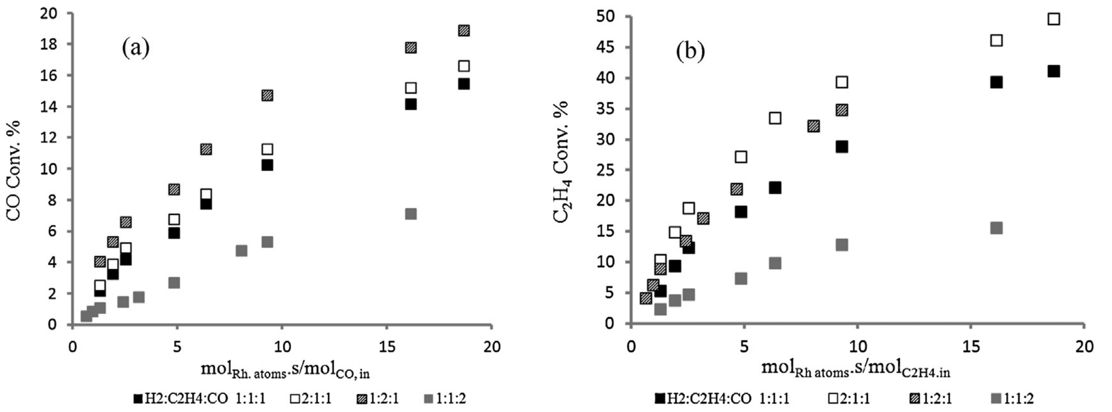

Fig. 10. CO and C_2H_4 conversions versus space time. Reaction conditions: catalyst 5%Rh on Al_2O_3, temperature, 473 K; pressure, 2.0 MPa.

to a significantly higher ethylene conversion but only to a slightly higher CO conversion.

Increasing the inlet CO concentration as it is depicted in Fig. 10a and b has a considerably negative effect on both the CO as the ethylene conversion. This can be understood if CO is the most abundant surface species and, hence; if the higher CO surface concentration results in a more pronounced decrease of the H_2 and C_2H_4 concentrations on the catalyst surface, such that both hydroformylation and hydrogenation rates decrease.

These results were in line with what Balakos et al. reported for dependence of the reaction rates on the partial pressures of reactants [9]. They observed both ethane and propanal formation rates are negative order in CO while positive order in both hydrogen and ethylene in heterogeneous hydroformylation on Rh/SiO_2 at 0.1 MPa and 513 K.

5. Conclusions

Gas phase hydroformylation on 5%Rh on Al_2O_3, 1%Co on Al_2O_3 and 0.5%Co–0.5%Rh on Al_2O_3 practically exclusively resulted in ethane, propanal and propanol formation. Finely dispersed Rh particles were the most active and selective (up to 45%) in ethylene hydroformylation to propanal and propanol. Structure sensitivity in ethylene hydroformylation has been explicitly observed for Co based catalysts: finer Co particles appear to be more active and selective than larger ones.

Irrespective of the investigated catalyst, the temperature effect is more pronounced on ethylene hydrogenation than on hydroformylation. The 15–20 kJ mol^{-1} higher apparent activation energy for ethane than for propanal formation is a result of the higher heat of chemisorption for CO than for hydrogen. CO was found to be the most abundant surface intermediate, resulting in an inhibiting effect on both hydroformylation and hydrogenation. Surface concentrations of hydrogen and ethylene were lower and did not result in inhibition effects within the investigated range of operating conditions. An ideal catalyst for ethylene hydroformylation must consist of a finely dispersed metal such as Rh with a maximum activity at temperatures below 483 K.

List of symbols

Cat.	catalyst
Conv.	conversion (%)
d_{at}	atomic diameter of given metal (m)
$d_{rel(VS)}$	the mean relative size of metallic crystallites
d_{VS}	the mean size of crystallite (m)
E_a	activation energy (kJ mol^{-1})
EDX	energy dispersive X-ray
$F_{A,0}$	molar inlet flow rate of A (mol/s)
F_p	molar outlet flow rate of P (mol/s) fraction of exposed metal
FE	atoms (%)
in	inlet
M	metal atoms
M_M	standard atomic weight (kg/mol)
S_p	selectivity towards product P (%)
TCD	thermal conductivity detector
TEM	transmission electron microscopy
TPD	temperature programmed desorption
TPR	temperature programmed reduction
XRD	X-ray diffraction

Acknowledgments

The research leading to these results has received funding from the European Community's Sixth Framework Programme (contract nr. 515792-2) and the Long Term Structural Methusalem Funding by the Flemish Government.

The authors would like to thanks Hilde Poelman, Vladimir Galvita and Vitaliy Bliznuk for assisting in XRD and TEM analysis.

References

[1] B. Cornils, M. Rasch, Angew. Chem. Int. Ed. 33 (1994) 2144–2163.
[2] P.W. Van Leeuwen, Rhodium Catalyzed Hydroformylation, Springer, New York, 2002.
[3] B. Breit, W. Seiche, Synthesis (2001) 1–36.
[4] K. Otsuka, T. Ando, I. Yamanaka, J. Catal. 165 (1997) 221–230.
[5] B. Cornils, Applied Homogeneous Catalysis with Organometallic Compounds, VCH, Weinheim, 1996.
[6] T.A. Zeelie, A. Root, A.O.I. Krause, Appl. Catal., A 285 (2005) 96–109.
[7] Ullmann's Encyclopedia of Industrial Chemistry, sixth ed., John Wiley & Sons, 2002.
[8] T.A. Zeelie, Rhodium and Cobalt Catalysts in the Heterogeneous Hydroformylation of Ethane, Propene and 1-Hexene, 2007, Helsinki (PhD thesis).
[9] M.W. Balakos, S.S.C. Chuang, J. Catal. 151 (1994) 266–278.
[10] U.J. Jauregui-Haza, O. Diaz-Abin, A.M. Wilhelm, H. Delmas, Ind. Eng. Chem. Res. 44 (2005) 9636–9641.
[11] K. Tomishige, I. Furikado, T. Yamagishi, S. Ito, K. Kunimori, Catal. Lett. 103 (2005) 15–21.
[12] M.A. Brundage, M.W. Balakos, S.S.C. Chaung, J. Catal. 173 (1998) 122–133.
[13] V.I. Zapirtan, B.L. Mojet, J.G.V. Ommen, J. Spitzer, L. Lefferts, Catal. Lett. 101 (1–2) (2005) 43–47.
[14] T. Hanaoka, H. Arakawa, T. Matsuzaki, Y. Sugi, K. Kanno, Y. Abe, Catal. Today 58 (2000) 271–280.
[15] F.S. Xiao, M. Ichikawa, J. Catal. 147 (1994) 578–593.
[16] C.U. Pittman Jr., G.M. Wilemon, J. Org. Chem. 46 (1981) 1901–1905.
[17] W. Junfan, S. Juntan, L. Hong, H. Binglin, React. Polym. 12 (1990) 177–186.
[18] D. Evans, J.A. Osborn, G. Wilkinson, J. Chem. Soc. 12 (1968) 3133–3142.
[19] W.A. Dietz, J. Gas Chromatogr. 5 (1967) 68–71.
[20] A. Borodzinski, M. Bonarowska, Langmuir 13 (1997) 5613–5620.
[21] R.J. Berger, E.H. Stitt, G.B. Marin, F. Kapteijn, J. Moulijn, CATTECH 5 (2001) 30–60.

[22] M.A. Brundage, S.S.C. Chaung, J. Catal. 164 (1996) 94–108.
[23] G. Henrici-Olive, S. Olive, The Chemistry of Catalyzed Hydrogenation of Carbon Monoxide, Springer-Verlag, Heidelberg, 1980.
[24] C.D. Frohning, C.W. Kohlpainter, in: B. Cornils, W.A. Herrmann (Eds.), Applied Homogeneous Catalysts with Organometallic Compounds, VCH, Weinheim, 1996 (Chapter 2.1).
[25] J.P. Hindermann, G.J. Hutchings, A. Kiennemann, Catal. Rev. 35 (1993) 1–127.
[26] P. Biloen, W.M.H. Sachtler, Adv. Catal. 30 (1981) 165–216.
[27] G. Lozano-Blanco, J.W. Thybaut, K. Surla, P. Galtier, G.B. Marin, Oil Gas Sci. Technol. Rev. IFP 61 (2006) 489–496.
[28] G.L. Bezemer, J.H. Bitter, H.P.C.E. Kuipers, H. Oosterbeek, J.E. Holewijn, X. Xu, F. Kapteijn, A.J. van Dillen, K.P. de Jong, J. Am. Chem. Soc. 128 (2006) 3956–3964.
[29] H. Pichler, H. Schulz, Chem. Ing. Tech. 42 (1970) 1162–1174.
[30] G. Lozano-Blanco, J.W. Thybaut, K. Surla, P. Galtier, G.B. Marin, Ind. Eng. Chem. Res. 47 (2008) 5879–6589.